THE MOST LIKELY SOURCES OF HIGH-ENERGY COSMIC-RAY ELECTRONS IN SUPERNOVA REMNANTS

T. KOBAYASHI

Department of Physics, Aoyama Gakuin University, Sagamihara 229-8558, Japan; tadasi-k@deneb.phys.aoyama.ac.jp

Y. KOMORI

Kanagawa University of Human Services, Yokosuka 238-0013, Japan; komori-y@kuhs.ac.jp

K. YOSHIDA

Faculty of Engineering, Kanagawa University, Yokohama 221-8686, Japan; yoshida@kit.ie.kanagawa-u.ac.jp

AND

J. NISHIMURA

Institute of Space and Astronautical Science, Sagamihara 229-8510, Japan; nisimura@icrr.u-tokyo.ac.jp

ABSTRACT

Evidence of nonthermal X-ray emission and TeV gamma rays from supernova remnants (SNRs) have strengthened the hypothesis that primary Galactic cosmic-ray electrons are accelerated in SNRs. High-energy electrons lose energy via synchrotron and inverse Compton processes during propagation in the Galaxy. Because of these radiative losses, TeV electrons liberated from SNRs at distances larger than $\sim$1 kpc, or times older than $\sim$10^5 yr, cannot reach the solar system. We investigated the cosmic-ray electron spectrum observed in the solar system using an analytical method and considered several candidate sources among nearby SNRs that may contribute to the high-energy electron flux. In particular, we discuss the effects for the release time from SNRs after the explosion, as well as the deviation of a source spectrum from a simple power law. From this calculation, we found that some nearby sources, such as Vela, Cygnus Loop, or Monogem, could leave unique signatures in the form of identifiable structure in the energy spectrum of TeV electrons and show anisotropies toward the sources, depending on when the electrons were liberated from the remnant. This suggests that, in addition to providing information on the mechanisms of acceleration and propagation of cosmic rays, specific cosmic-ray sources can be identified through the precise electron observation in the TeV region.

Subject headings: acceleration of particles — cosmic rays — gamma rays: theory — supernova remnants

1. INTRODUCTION

Radio observations have indicated that supernova remnants (SNRs) are the most likely sources of cosmic-ray electrons in the energy region below $\sim$10 GeV. Evidence for nonthermal X-ray emission from the supernova remnant SN 1006 discovered with the *ASCA* satellite (Koyama et al. 1995) strongly supports the hypothesis that Galactic cosmic-ray electrons in the TeV region originate in supernovae. In this case, TeV gamma rays should be produced via the inverse Compton process between accelerated electrons and the cosmic microwave background (CMB) radiation, and indeed TeV gamma rays were detected by the CANGAROO experiment (Tanimori et al. 1998). Additional evidence for X-ray synchrotron emission is provided by observations of several other SNRs, such as RX J1713.7−3946 (Koyama et al. 1997), Cas A (Allen et al. 1997), IC 443 (Keohane et al. 1997), G374.3−0.5 (Slane et al. 1999), and RX J0852.0−4622 (Slane et al. 2001). In SNR RX J1713.7−3946, evidence for the acceleration of cosmic-ray protons is reported by Enomoto et al. (2002) from TeV gamma-ray observations. However, there are also arguments that the TeV gamma rays observed cannot be interpreted as hadronic in origin (Reimer & Pohl 2002; Butt et al. 2002).

To clarify the origins of cosmic rays and their propagation mechanisms within the Galaxy, electrons provide an ideal probe, complementary to the nucleonic component because of their low mass and leptonic nature. High-energy electrons lose energy primarily via synchrotron and inverse Compton processes during propagation in the Galaxy. These processes, combined with the absence of hadronic interactions, simplify modeling of the propagation of electrons compared with other cosmic-ray components such as nucleons. Since the energy-loss rate is almost proportional to E^2, higher energy electrons lose energy more rapidly. TeV electrons lose most of their energy on a timescale of $\sim$10^5 yr, and their propagation distances are therefore limited to several hundred parsecs.

Measurements of cosmic-ray electrons in the TeV region have been successfully performed only with emulsion chamber detectors (Nishimura et al. 1980; Kobayashi et al. 1999). The observed energy spectra extend without cutoff up to $\sim$2 TeV. This means that the observed TeV electrons must have been accelerated in SNRs at distances within several hundred parsecs, and at times within $\sim$10^5 yr ago.

Several models have been proposed to describe cosmic-ray propagation in the Galaxy, motivated by attempts to fit existing data on the heavy primary composition and spectra of different species assuming the same simple power-law source spectrum. Among these models, it is believed that the diffusion model provides the most realistic description of the propagation. The solution for the electron density in the diffusion equation is derived by several authors (e.g., Jokipii & Meyer 1968; Ginzburg & Ptuskin 1976; Nishimura et al. 1979; Berezinskii et al. 1990 and references therein), under different boundary conditions for the Galactic halo.

In a study of the propagation of cosmic-ray electrons, Shen (1970) first pointed out that a continuous source distribution

model is not valid in the energy region above 100 GeV, because the electron spectrum in that energy range depends on the age and distance of a few local sources. He showed that high-energy electrons over 100 GeV probably come from the Vela X pulsar and predicted a cutoff at $\sim$2 TeV in the energy spectrum. Although various parameters for SNRs and diffusion coefficients were not known very well at that time, the concept proposed by the author has been accepted in later works.

Cowsik & Lee (1979) have investigated the electron spectrum in terms of contributions from discrete sources such as SNRs distributed over the Galaxy. Their calculations apply in the case of sources continuously active in time. They suggested that such sources must be located within a few hundred parsecs of the solar system to prevent radiative energy losses from inducing a premature cutoff in the energy spectrum. They took the diffusion coefficient $D = 10^{28}$ cm^2 s^{-1}, independent of energy, which is much smaller than recently accepted values in the energy region over 100 GeV (see § 2.2). They concluded that it is very unlikely that SNRs are the only sources of cosmic-ray electrons in the energy range 1 GeV to 1 TeV, but this result seems due to the inappropriate value of the diffusion coefficient assumed by themselves.

Nishimura et al. (1979) calculated the propagation of electrons from SNRs, using a solution of the diffusion equation with a disk-shaped boundary condition. They showed that the TeV electron spectrum would deviate from power-law behavior because of fluctuations caused by the small number of sources capable of contributing to the observed flux in the TeV region.

To explain the features of both energy spectrum and charge composition of electrons, Aharonian et al. (1995) suggested an approach that separates the contribution of one nearby source, with age 10^5 yr and distance 100 pc, from the contributions of other Galactic sources at distances over 1 kpc. Using this approach, Atoyan et al. (1995) calculated the electron energy spectrum in analytical form. They considered the energy-dependent diffusive propagation of electrons, assuming the diffusion coefficient $D = 7 \times 10^{27}$ cm^2 s^{-1} at 10 GeV, increasing with energy as $E^{0.6}$. They showed that the observed energy spectrum from sub-GeV to TeV energies can be explained by this model.

Pohl & Esposito (1998) have pointed out that if cosmic-ray electrons are accelerated in SNRs, the observed electron spectrum should be strongly time-dependent above 30 GeV as a result of Poisson fluctuations in the number of SNRs within a given volume and time interval. They assumed the diffusion coefficient $D = 4 \times 10^{27}(E/1 \text{ GeV})^{0.6}$ cm^2 s^{-1} and calculated 400 cases of spectra using a random distribution of SNRs in space and time. They argued that in their model, an injection spectral index of 2.0 cannot be rejected for the observed local electron flux at high energy, with a probability of 5% over all their calculated spectra.

Erlykin & Wolfendale (2002) considered the model for cosmic-ray electron production in the supernova explosion and variants for the subsequent propagation. In their model, electrons are accelerated throughout the SNR lifetime of several 10^4 yr, and after the cessation of the acceleration process electrons leave the remnant. They simulated the electron spectra by taking the random distribution of SNe in the Galaxy and letting the electrons diffuse to the solar system.

As pointed out in these works, at energy higher than $\sim$1 TeV, the propagation lifetime of electrons is so short that only a few cosmic-ray sources can contribute to the observed flux. Thus, one expects fluctuations in the local electron energy spectrum reflecting the contributions of this small number of discrete sources. To analyze fluctuations in the spectrum, we use the method of separating the contributions of distant and nearby sources to the total flux of high-energy electrons. Although this approach was discussed by earlier authors (e.g., Atoyan et al. 1995 and references therein), the main difference between the present and earlier works is that in this paper we took only known, observed local SNRs as nearby sources. Using information on the ages and distances of observed SNRs in the neighborhood of the solar system, we could determine which sources contribute electrons most efficiently in a given energy range and thus correlate individual sources with features of the electron spectrum. In addition, one would expect the high-energy electron flux to be anisotropic if the most significant sources are nearby (Shen & Mao 1971; Ptuskin & Ormes 1995). This means that we can identify cosmic-ray electron sources from the analysis of the local electron spectrum together with anisotropies in arrival direction.

For this purpose, we calculated the electron energy spectra with the diffusion model in a semianalytic approach, separating the contributions of distant and nearby sources. In this calculation, we particularly took into account the effects of the delay of electron liberation from SNRs after the explosion, as well as the deviation from a single power-law spectrum of electrons in SNRs. As a result, we indicate that nearby SNRs such as the Vela, Cygnus Loop, or Monogem are the most likely candidates for the sources of cosmic-ray electrons in the TeV region, depending on when the electrons were released from SNRs. If these sources are proven to be the main contributors of high-energy electrons, we can precisely analyze the propagation of TeV electrons by comparing predicted results with observed electron spectra, and the degree of anisotropy in the direction of the sources. Such analyses will yield more detailed information about the acceleration and propagation of cosmic rays.

2. ACCELERATION IN SNRs AND PROPAGATION IN THE GALAXY

2.1. *Accelerated Electrons in SNRs and Their Liberation Time*

According to shock-acceleration models, the maximum energy of accelerated electrons is limited by the SNR age, a free escape from the shock region of MHD turbulence, or synchrotron losses (Sturner et al. 1997; Reynolds 1996). Analysis of the observed radio and X-ray spectra also indicates that the typical electron spectrum produced in a remnant is a power law with a cutoff of $\sim$10–100 TeV (Reynolds & Keohane 1999; Hendrick & Reynolds 2001). Therefore, we approximate an electron injection spectrum of a power law with an exponential cutoff of the form of $\exp(-E/E_c)$, as taken by these authors.

As discussed in Erlykin & Wolfendale (2002), it is also important to take into account when the accelerated electrons are liberated from the remnant after the explosion. From shock-acceleration theory, it is suggested that the electrons are liberated from SNRs in the termination of the shock, i.e., when the shock velocity has dropped to the mean interstellar medium (ISM) Alfvén velocity and the remnant has been reduced in the ISM (e.g., Dorfi 2000). This timescale is $\sim$10^5 yr. However, there is no clear observational evidence for the release time of the TeV electrons from SNRs. In the scenario of the SNR origin of cosmic-ray electrons, the accelerated TeV electrons should be liberated from the remnant within $\sim$10^5 yr, or the acceleration process should operate until the last phase of SNRs. This is because the lifetime of TeV electrons in the remnant is estimated to be less than a few times of 10^4 yr because of

synchrotron loss inside SNRs with a magnetic field of 10 μG. Therefore, we evaluated the cosmic-ray electron spectra, changing the electron release time τ from 0 to 1×10^5 yr.

2.2. Properties of the Propagation of High-Energy Electrons

High-energy electrons above 10 GeV lose their energy mainly via the synchrotron and inverse Compton processes while propagating through the Galaxy. The energy-loss rate is given by

$$-\frac{dE}{dt} = bE^2, \qquad (1)$$

with

$$b = \frac{4\sigma c}{3(mc^2)^2}\left(\frac{B^2}{8\pi} + w_{\rm ph}\right). \qquad (2)$$

Here E is the electron energy, m is the mass of electron, c is the speed of light, B is the magnetic field strength in the Galaxy, $w_{\rm ph}$ is the energy density of interstellar photons, and σ is the cross section for Thomson scattering. Equation (2) is valid when the inverse Compton process is well approximated by the Thomson scattering cross section, but we need corrections from the Klein-Nishina formula for high-energy electrons as described below.

Typically quoted values for the interstellar magnetic field are estimated from measurements of the Zeeman splitting, the Faraday rotation, or the radio synchrotron emission. The estimates from Zeeman splitting and Faraday rotation measurements refer only to the line-of-sight component of the magnetic field. They are also biased toward cold neutral and warm ionized regions, respectively. Using the radio synchrotron emission from relativistic electrons, the local magnetic field strength of $B_\perp \simeq 5$ μG is obtained as a more adequate value (Ferriere 2001). Here $B_\perp$ means the magnetic field perpendicular to the electron velocity, that is, $B_\perp^2 = 2B^2/3$. In this calculation, we adopted $B_\perp = 5$ μG for our Galaxy.

Since the Thomson scattering cross section approximation is inadequate for high-energy electrons, we evaluate the energy-loss coefficient b using the Compton scattering cross section in the following. The interstellar radiation field in the Galaxy is dominated by three components: 2.7 K CMB, reemitted radiation from dust grains, and stellar radiation. The energy densities of photons are 0.26 eV cm^{-3} for CMB, 0.20 eV cm^{-3} for reemitted radiation from dust grains, and 0.45 eV cm^{-3} for stellar radiation, respectively (Mathis et al. 1983). For inverse Compton scattering, we calculated the Klein-Nishina cross section accurately using the formula by Blumenthal & Gould (1970). The resulting energy-loss coefficient b decreases gradually with energy, as shown in Figure 1, where the radiation field is assumed to be isotropic. For electrons in the TeV region, energy loss through interactions with the CMB dominates over the other two components.

In a diffusive propagation model, the diffusion coefficient determines the travel distance of electrons in a given time. The diffusion coefficient D has been estimated by using the observed ratios of secondary to primary nuclei (B/C) by *HEAO-C* (Engelmann et al. 1990) and *Voyager* (Lukasiak et al. 1994) and is given by

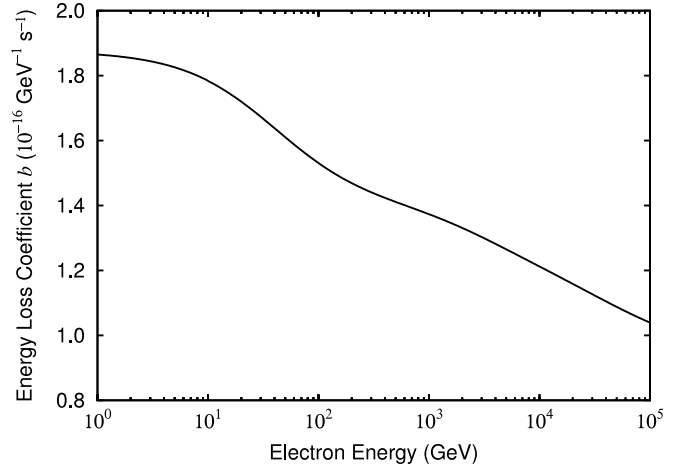$$D = 2 \times 10^{28}(E/5 \text{ GeV})^\delta \text{ cm}^2 \text{ s}^{-1}, \qquad (3)$$

FIG. 1.—Energy-loss coefficient of cosmic-ray electrons in the Galaxy with energy. The magnetic field is assumed to be $B_\perp = 5$ μG.

where

$$\delta = \begin{cases} 0 & E < 5 \text{ GeV}, \\ 0.6 & E \geq 5 \text{ GeV}. \end{cases}$$

Equation (3) agrees well with the experimental data up to tens of GeV. Beyond 100 GeV, there have been scarcely data on B/C until quite recently, and it was not clear whether equation (3) is applicable to the higher energy region or not.

There are arguments that simple extrapolation of $D \propto E^\delta$ with $\delta = 0.6$ gives too large a diffusion coefficient in the 1–100 TeV region to interpret the observed anisotropy of primary cosmic-rays less than 10^{-3} (Ambrosio et al. 2003 and references therein). Thus, it has been argued that the increase of the diffusion coefficient with energy should become slower than $\delta = 0.6$ at somewhere beyond tens of GeV, and also that $\delta = 0.3$ is plausible from a Kolmogorov-type spectrum of turbulence in the ISM (e.g., Gaisser 1990, 2000; Jones et al. 2001). In fact, recent work on emulsion chamber experiments with long balloon exposures has shown data of B/C and (secondary species of Fe)/Fe in the TeV region, which indicate that the diffusion coefficient is consistent with the change of δ from 0.6 to 0.3 between tens of GeV and 1 TeV (Furukawa et al. 2003).

Hence, we take $D = (2-5) \times 10^{29}(E/\text{TeV})^{0.3} (\text{cm}^2 \text{ s}^{-1})$ as a plausible diffusion coefficient in TeV region. The numerical values of 2 and 5 are derived from the assumption that equation (3) is valid up to 50 GeV or 1 TeV, respectively. With this assumption, the source spectral index γ is chosen to maintain $\gamma + \delta = 2.7$.

Since high-energy electrons lose energy by synchrotron and inverse Compton processes at the rate $dE/dt = -bE^2$, electrons lose almost all of their energy E after time $T = 1/bE$. Therefore, electrons observed with energy E must have been accelerated within $T = 1/bE$ from the present. Hence, the lifetime T becomes progressively shorter with increasing energy. Assuming $B_\perp = 5$ μG and taking the Klein-Nishina formula for Compton process, the lifetime is $T = 1/bE \simeq 2.5 \times 10^5$ yr/E TeV. As an approximate treatment, electrons can diffuse a distance of $R = (2DT)^{1/2}$ during this time, i.e., 0.6–0.9 kpc for $D = (2-5) \times 10^{29}$ cm^2 s^{-1} at 1 TeV. A more precise estimate for R is given in the following section.

2.3. *Propagation of Cosmic Rays from a Single Source*

In the diffusion model for the propagation of electrons in the Galaxy, the electron density N_e is given by the equation

$$\frac{dN_e}{dt} - \nabla(D\nabla N_e) - \frac{\partial}{\partial E}(bE^2 N_e) = Q, \qquad (4)$$

where Q is the electron source strength. This equation is valid for the isotropic part of the electron distribution and justified when the anisotropic part is relatively small.

We take into account the fact that the Galactic disk, where the sources are distributed, is surrounded by a halo in which the cosmic rays are confined for a long time before they escape into intergalactic space. We assume that cosmic-ray electrons are bounded by two parallel planes at $z = \pm h$, with the median plane being occupied by the Galactic disk. The halo thickness, h, is estimated to be $2.8^{+1.2}_{-0.9}$ kpc from ^{10}Be observations from the High-Energy Telescope (HET) aboard the *Voyager 1* and *Voyager 2* spacecrafts (Lukasiak et al. 1994), which is also consistent with the observed Galactic radio emission structure (Beuermann et al. 1985). Thus, we need to consider solutions with these boundary conditions for further analysis. Assuming burstlike injection of electrons after the supernova explosion, the source term can be represented by

$$Q(E, \rho, z, t) = Q(E)\delta(\rho)\delta(z)\delta(t), \qquad (5)$$

where ρ is the cylindrical distance to a source from the solar system. Since the solar system is located at $z = 15$ pc, quite near the median plane of the disk, and the sources are uniformly distributed in a layer much thinner than the confinement domain, we set $z = 0$ hereafter. The density of electrons, N_e, from a point source with injection spectrum

$$Q(E) = Q_0 E^{-\gamma} \exp(-E/E_c), \qquad (6)$$

at a distance ρ and time t after the release of electrons from the remnant, is derived from the diffusion equation using the Fourier transform, assuming the diffusion coefficient has the form $D = D_0 E^\delta$. Taking the boundary condition $N_e = 0$ at the boundary of the Galactic halo $z = \pm h$, the general solution of equation (4) in cylindrical coordinates is given by

$$N_e(E, \rho, t) = \sum_{n=0}^{\infty} \left\{ \frac{Q_0}{4\pi D_1 h} \exp\left(-D_1 k_n^2 - \frac{\rho_2}{4D_1}\right) \right.$$
$$\left. \times (1 - bEt)^{\gamma-2} E^{-\gamma} \exp\left[-\frac{E}{E_c(1-bEt)}\right] \right\}, \quad (7)$$

where

$$D_1 = \int_E^{E/(1-bEt)} (1/b)DE^{-2}\, dE = \frac{D_0\left[1 - (1-bEt)^{1-\delta}\right]}{b(1-\delta)E^{1-\delta}},$$

and

$$k_n = \frac{\pi}{2h}(2n+1).$$

2.4. *Distant Components and Nearby Components*

Integrating $N_e(E, \rho, t)$ of solution (7) with ρ from 0 to ∞, we derive

$$N_e(E, t) = \int_0^\infty N_e(E, \rho, t)2\pi\rho\, d\rho$$
$$= \sum_{n=0}^\infty \left\{ \frac{Q_0}{h} \exp(-D_1 k_n^2)(1-bEt)^{\gamma-2}E^{-\gamma} \right.$$
$$\left. \times \exp\left[-\frac{E}{E_c(1-bEt)}\right] \right\}. \qquad (8)$$

In this calculation, we approximated the integration on ρ to range from 0 to ∞. Since electrons cannot propagate to larger distances than the halo thickness of h in the radial direction, we can ignore the effects of the lateral distribution of the sources on the Galactic disk. In integrating $N_e(E, t)$ of equation (8) on t from 0 to $1/bE$, we need the numerical integration. In the case of $E \ll E_c$, however, we can perform the integration in an analytical way, since the exponential cutoff term can be ignored. The solution is given by a confluent hypergeometric function for each term in the series.

$$N_e(E) = \int_0^{1/(bE)} fN_e(E, t)\, dt$$
$$= \sum_{n=0}^\infty fQ_0 \frac{{}_1F_1[1, (\gamma-\delta)/(1-\delta), -y]}{hb(\gamma-1)E^{\gamma+1}}, \qquad (9)$$

where ${}_1F_1$ is a confluent hypergeometric function and

$$y = D_0 \frac{k_n^2}{(1-\delta)bE^{1-\delta}},$$

and f is the supernova explosion rate in the Galaxy per unit area and unit time. This analytic form is convenient to sum up many terms in the series. Higher energy electrons cannot reach the halo boundary because of their larger energy-loss rate and distribute around the Galactic disk plane. Therefore, we need to include the higher order Fourier components to estimate the flux of higher energy electrons. In fact, we need to add up to 10 terms at 10 GeV and up to 2×10^2 terms at 10 TeV to get a precision of a few percent in the convergence of the series solution (9). In order to simplify the calculation for the high-energy region, we can use a three-dimensional solution without boundary conditions instead of the two-dimensional solution (9), which is given by

$$N_e(E, r, t) = \frac{1}{(4\pi D_1)^{3/2}} e^{-r^2/(4D_1)} Q\left(\frac{E}{1-bEt}\right)$$
$$\times (1-bEt)^{-2} \exp\left[-\frac{E}{E_c(1-bEt)}\right] \qquad (10)$$

(e.g., Berezinskii et al. 1990 and references therein), where r is the radial distance to a source from the solar system, and

$$D_1 = \int_E^{E/(1-bEt)} (1/b)DE^{-2}\, dE.$$

The accuracy obtained by this approximation is discussed in Appendix A.

The flux of electrons from sources continuously and uniformly distributed in the Galactic disk is derived from the integration of electron density with respect to ρ and t in

$$J(E) = \frac{c}{4\pi} N_e(E). \tag{11}$$

In the low-energy region, below 1 TeV, many sources contribute to the observed electron flux. As the energy of the observed electrons increases, the number of electron sources decreases, and only nearby sources can contribute to the electron flux. As described in § 2.2, nearby young cosmic-ray electron sources create discrete effects in the TeV region, such as structure in the electron spectrum and the anisotropy favoring the source direction. Thus, we can define the contribution from distant or relatively old sources by subtracting the flux of nearby young sources, eliminating the effects of fluctuations due to the small number of nearby sources, as follows:

$$J_d(E) = J(E) - J_n(E), \tag{12}$$

where J_d and J_n show the flux of electrons from distant (in spacetime) and nearby sources, respectively. Here we calculated the contribution of nearby sources distributed uniformly in space and time as

$$J_n(E) = \frac{c}{4\pi} \int_0^{T_0} dt \int_0^{R_0} d\rho \, f N_e(E, \, \rho, \, t) 2\pi\rho. \tag{13}$$

Appropriate values of R_0 and T_0 are discussed in § 4.2.

3. SNRs AS COSMIC-RAY ELECTRON SOURCES

As described in § 1, recent X-ray and TeV gamma-ray observations indicate that high-energy electrons are accelerated in SNRs. Here we assumed that SNRs are cosmic-ray electron sources, and that electrons are liberated at once from SNRs at the time of $\tau = 0$, 5×10^3, 1×10^4, 5×10^4, and 1×10^5 yr after the explosion. As described in § 4, the case of the continuous release is well approximated by the burstlike release with a mean value of the liberation time.

From the observations of SN 1006 (Reynolds 1996; Koyama et al. 1995; Tanimori et al. 1998), the output energy in electrons above 1 GeV is estimated to be $\sim 1 \times 10^{48}$ ergs. We can also estimate the net output energy for electrons from supernovae using the energy density of cosmic rays and the supernova rate of 1/30 yr in the Galaxy (Berezinskii et al.

1990; Gaisser 2000 and other references therein). The output energy of electrons above 1 GeV estimated in this way is about 10^{48} ergs per SN and is consistent with the estimate from SN 1006. Therefore, we took the output energy from a supernova in electrons above 1 GeV to be $W = 1 \times 10^{48}$ ergs.

To analyze contributions due to discrete cosmic-ray electron sources, we list in Table 1 all known SNRs that are located within 1 kpc of the solar system and with an age less than 4×10^5 yr. For each source, the maximum energy $E_{\max}$ of electrons reaching the solar system is given by $E_{\max} = 1/(bT)$, with the energy-loss coefficient b shown in Figure 1 and the age T of each SNR, which are determined independent of the diffusion coefficient.

Distance to SNRs is an important parameter in evaluating the high-energy electron flux, and we comment on this parameter of some SNRs listed in Table 1. So far, the canonical distance to the Vela SNR has been taken to be 500 pc, a value that was derived from the analysis of its angular diameter in comparison with the Cygnus Loop and IC 443 (Milne 1968), and pulsar dispersion determination (Taylor & Cordes 1993). However, recent parallax measurements clearly indicate that the distance of 500 pc is too large. Cha et al. (1999) obtained a high-resolution Ca II absorption line toward 68 OB stars in the direction of the Vela SNR. The distances to these stars were determined by trigonometric parallax measurements with the *Hipparcos* satellite and spectroscopic parallaxes based on photometric colors and spectral types. The distance to the Vela SNR is constrained to be 250 ± 30 pc because of the presence of the Doppler spread Ca II absorption line attributable to the remnant along some lines of sight. Caraveo et al. (2001) also applied high-resolution astrometry to the Vela pulsar (PSR B0833−45) $V \sim 23.6$ optical counterpart. Using *Hubble Space Telescope* (*HST*) observations, they obtained the first optical measurement of the annual parallax of the Vela pulsar, yielding a distance of 294^{+76}_{-50} pc. Therefore, we calculate the electron flux adopting a distance of 300 pc to the Vela SNR.

Previously, a distance of 770 pc to the Cygnus Loop was often quoted (Minkowski 1958). Recently, Blair et al. (1999) suggested that the distance is 440^{+130}_{-100} pc, based on *HST* observations of a filament in the remnant. Thus, we took the distance to be 440 pc, considerably smaller than the previously quoted distance of 770 pc.

For the recently discovered SNR RX J0852.0−4622, the estimated age of ~ 680 yr and distance of ~ 200 pc were based on thermal X-ray emission and ^{44}Ti gamma-ray detection

TABLE 1
LIST OF NEARBY SNRs

SNR	Distance (kpc)	Age (yr)	$E_{\max}$[a] (TeV)	Reference
SN 185	0.95	1.8×10^3	1.7×10^2	1
S147	0.80	4.6×10^3	63	2
HB 21	0.80	1.9×10^4	14	3, 4
G65.3+5.7	0.80	2.0×10^4	13	5
Cygnus Loop	0.44	2.0×10^4	13	6, 7
Vela	0.30	1.1×10^4	25	8
Monogem	0.30	8.6×10^4	2.8	9
Loop1	0.17	2.0×10^5	1.2	10
Geminga	0.4	3.4×10^5	0.67	11

[a] Maximum energy limited by the propagation of electrons in the case of the prompt release after the explosion. The delay of the release time gives the larger value.

REFERENCES.—(1) Strom 1994; (2) Braun et al. 1989; (3) Tatematsu et al. 1990; (4) Leahy & Aschenbach 1996; (5) Green 1988; (6) Miyata et al. 1994; (7) Blair et al. 1999; (8) Caraveo et al. 2001; (9) Plucinsky et al. 1996; (10) Egger & Aschenbach 1995; (11) Caraveo et al. 1996.

(Aschenbach 1998; Iyudin et al. 1998). However, *ASCA* observations reveal that the X-ray emission is nonthermal, and reanalysis of the COMPTEL data indicates that the ^{44}Ti gamma-ray detection is only significant at the 2–4 σ level (Slane et al. 2001 and references therein). Thus, it is suggested that RX J0852.0−4622 is at a larger distance, 1–2 kpc (Slane et al. 2001), so we do not include it in Table 1.

4. RESULTS

4.1. *Electrons from the Known Nearby SNRs*

Figure 2 shows contours of the expected electron flux at 3 TeV (with flux values scaled by E^3) as a function of age and distance of the SNR. As described in the preceding section, we assumed that the output energy of electrons over 1 GeV is $W = 1 \times 10^{48}$ ergs per SN, and the injection spectrum is a power-law function with an exponential cutoff of the form of $\exp\left(-E/E_c\right)$. The diffusion coefficient has the form

$D = D_0(E/\text{TeV})^\delta$ cm^2 s^{-1}, where δ is 0.3 in the TeV region and the spectral index γ is chosen to maintain $\gamma + \delta = 2.7$. As shown in Figure 2, the electron flux is strongly dependent on source age and distance. In the case of the prompt release of electrons after the explosion, the flux from the Vela SNR is the largest among the known SNRs listed in Table 1. The flux value is quite sensitive to the change of distance to Vela from 500 to 300 pc, since the solution for electron density yields a Gaussian distribution function of a distance as shown in equations (7) or (10). The flux of electrons at a distance of 300 pc is 2 orders of magnitude larger than at 500 pc.

4.2. *Calculated Electron Energy Spectrum Compared with the Observed Spectrum*

We separately calculated the contributions to the electron energy spectrum from nearby and distant sources. We selected SNRs in the neighborhood of the solar system located within a distance of 1 kpc and an electron release time within 1×10^5 yr in the past. The boundary condition in this domain almost corresponds to the diffusion path length and lifetime of electrons around 1 TeV. We calculated the electron flux from nearby sources using the distance and ages of selected SNRs in Table 1 with equation (10). The justification for taking $R_0 = 1$ kpc and $T_0 = 1 \times 10^5$ yr is discussed in Appendix B. The SNRs in the nearby region are thus SN 185, S147, HB 21, G65.3+5.7, Cygnus Loop, Vela, and Monogem. In this calculation, we assumed that supernovae occur uniformly on the Galactic disk at the rate of 1/30 yr and took the halo thickness to be $h = 3$ kpc.

Figure 3 shows the calculated energy spectra of electrons without a cutoff of the injection spectrum in the case of prompt release after the explosion ($\tau = 0$), compared to the observed data (Golden et al. 1984, 1994; Tang 1984; Kobayashi et al. 1999; Boezio et al. 2000; DuVernois et al. 2001; Torii et al. 2001; Aguilar et al. 2002). Here we illustrate the cases of the diffusion coefficient of $D = D_0(E/\text{TeV})^{0.3}$ with $D_0 = 2 \times 10^{29}$cm^2 s^{-1} and $D_0 = 5 \times 10^{29}$ cm^2 s^{-1} in TeV region, with $D = 2 \times 10^{28}(E/5 \text{ GeV})^{0.6}$ cm^2 s^{-1} up to 50 GeV or 1 TeV as given by equation (3) in § 2.2. In this figure, we also plotted the flux of low-energy interstellar electrons estimated from the Galactic radio data (Rockstroh & Webber 1978). Cosmic-ray electrons have been observed by a variety of instruments, but only emulsion chamber data provide observations of electrons above 1 TeV. Since the flux of TeV electrons is low, detectors must have large acceptance $S\Omega$ and high proton rejection power ($\sim 10^5$). The emulsion chamber satisfies these requirements (Nishimura et al. 1980; Kobayashi et al. 1999).

Our propagation model, which consists of separately calculated distant and nearby components, is consistent with the observed data for the local primary electron spectrum in the energy range from 10 GeV to 2 TeV. Our model also predicts that nearby SNRs insert unique, identifiable structures in the electron spectrum from 1 to 10 TeV. As shown in Figure 3, the absolute flux and spectral shape change with the diffusion coefficient. On the other hand, the maximum energy of each SNR is the same, independent of the diffusion coefficient value, because it is determined by the age of the SNR.

We also calculated how the source spectral shape and release time of electrons from the remnant affect the cosmic-ray electron spectrum. We illustrate some examples of these calculations by taking $D_0 = 2 \times 10^{29}$ cm^2 s^{-1}. Figure 4 shows the calculated energy spectra with a cutoff of $E_c = 10$ TeV, 20 TeV, and ∞ in the injected electron spectrum, assuming the prompt release after the explosion. We can find that these spectra are similar to each other, independent of the cutoff
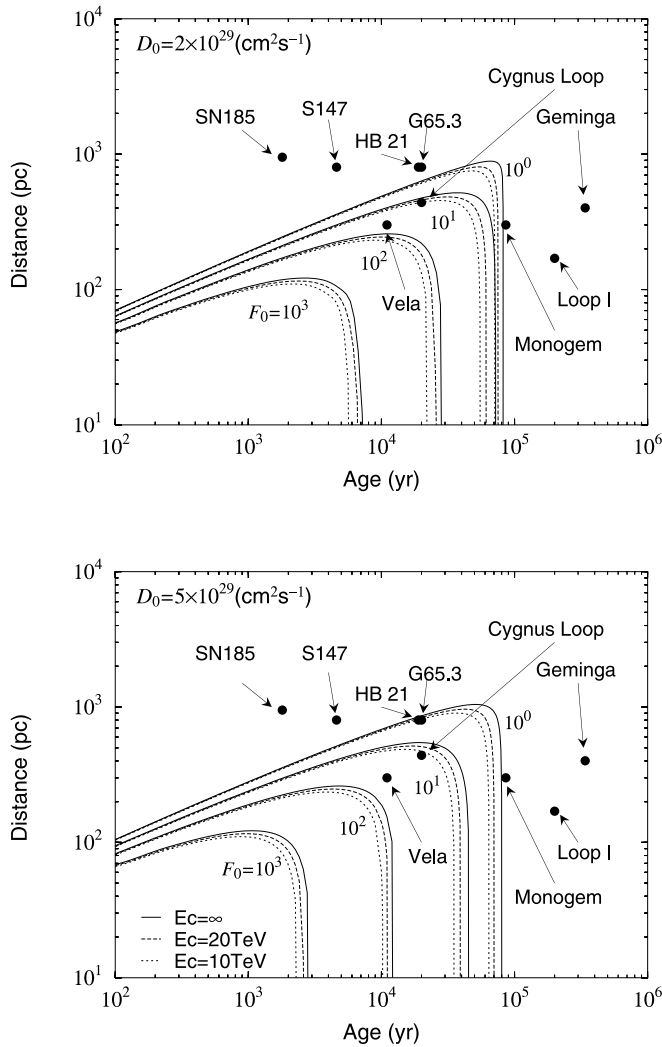
Fig. 2.—Contours of the electron flux at 3 TeV between distances and ages with the values of each SNR, in the case of the prompt release of electrons after the explosion. Lines show equal flux contour for $F_0 = (E/\text{GeV})^3 J$ GeV^2 m^{-2} s^{-1} sr^{-1}, where J is the flux of electrons at 3 TeV. Contour levels are 10^3, 10^2, 10^1, and 10^0 GeV^2 m^{-2} s^{-1} sr^{-1} with the output energy of electrons over 1 GeV of $W = 1 \times 10^{48}$ ergs per SN. Here the injection spectrum is a power law with an exponential cutoff of $E_c = 10$ TeV (*dotted line*), 20 TeV (*dashed line*), and ∞ (*solid line*). Upper and lower panels show the flux contours for $D = D_0 (E/\text{TeV})^{0.3}$ with $D_0 = 2 \times 10^{29}$ and $D_0 = 5 \times 10^{29}$ cm^2 s^{-1}, respectively.
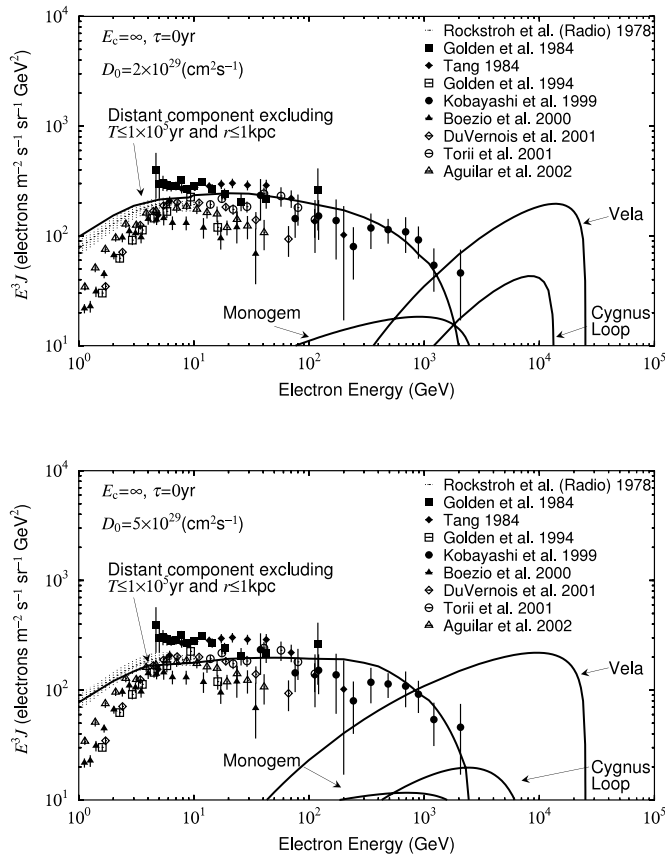
Fig. 3.—Calculated energy spectra of electrons without a cutoff of the injection spectrum for the prompt release after the explosion ($\tau = 0$), compared with presently available data. Here we took the diffusion coefficient of $D = D_0(E/\mathrm{TeV})^{0.3}$ with $D_0 = 2 \times 10^{29}$ cm^2 s^{-1} and $D_0 = 5 \times 10^{29}$ cm^2 s^{-1} in the TeV region, and $D = 2 \times 10^{28}(E/5 \, \mathrm{GeV})^{0.6}$ in the GeV region as given by eq. (3). See text for details.

energies. Figure 5 shows the calculated energy spectra with a cutoff of $E_c = 20$ TeV, in which electrons are released at once after the explosion in the release time of $\tau = 5 \times 10^3$, 1×10^4, 5×10^4, and 1×10^5 yr, respectively. As shown in this figure, it is to be noted that the spectrum for $\tau = 5 \times 10^3$ yr is almost the same with that of the prompt release after the explosion. However, the delay of the release time from SNRs has a large impact on the flux in the TeV region for $\tau \geq 1 \times 10^4$ yr.

We also checked the case of the continuous release. Figure 6 shows that these spectra are well represented by that of the burstlike release with a mean value of the continuous release time.

5. SUMMARY AND DISCUSSION

We calculated the energy spectrum of cosmic-ray electrons, separating the contributions of sources nearby in space and time (those within distances of 1 kpc and times of 1×10^5 yr) and Galactic sources located outside this domain.

There are only nine SNRs within a distance of 1 kpc and an age of 4×10^5 yr, as shown in Table 1, which is much smaller than the expected number of ~ 60 assuming a supernova rate of 1/30 yr and a Galactic disk radius of 15 kpc. This is due to selection biases in radio observations, since surface brightnesses in radio observations decrease with age. Thus, also coupled with the reason of the arguments in Appendix B, we

define a domain of $R \leq 1$ kpc and $T \leq 1 \times 10^5$ yr to evaluate the electron flux from nearby sources. There are seven known SNRs within this region listed in Table 1: Vela, Cygnus Loop, Monogem, G65.3+5.7, HB 21, S147, and SN 185. On the other hand, the expected number of SNRs in this smaller domain is ~ 15. The difference could be partly due to statistical fluctuations in the small number of sources, and it could also be due to undetected SNRs in this domain. In fact, the surface brightness estimated from an age of 1×10^5 yr, assuming adiabatic phase, is still fainter than the typical detection limit of surface brightness in studies of the distribution of Galactic SNRs (Kodaira 1974; Leahy & Xinji 1989). Although this indicates that the electron flux calculated from known nearby SNRs may give a lower limit of the flux, the contribution of undetected SNRs is expected to be relatively small in the case of the prompt release of electrons after the explosion. Since these undetected SNRs should have lower surface brightness and be older than detected SNRs, they could scarcely contribute to the electron intensity in the TeV region as indicated in Figure 2. Some quantitative arguments on this point are discussed in Appendix B.

Our model predicts that nearby SNRs, such as the Vela, Cygnus Loop, or Monogem, present unique, identifiable structures in the electron spectrum from 1 to 10 TeV. As the diffusion coefficient increases, electrons propagate larger distances with longer mean path length, resulting in the electron density becoming smaller. This causes a flatter spectral shape and smaller peak flux, as shown in Figure 3. The release time τ after the
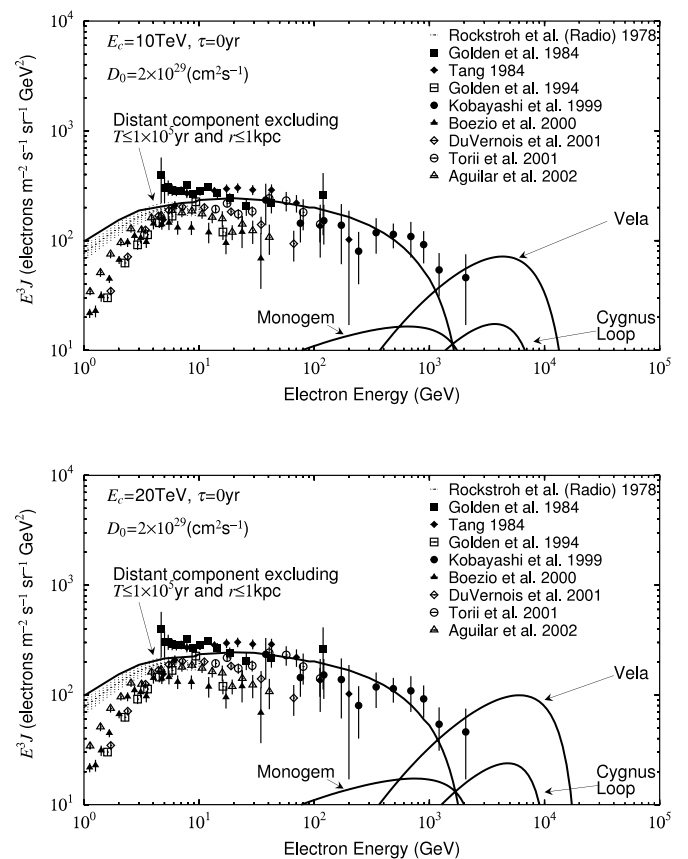

Fig. 4.—Calculated energy spectra with a cutoff of $E_c = 10$ and 20 TeV for the prompt release after the explosion ($\tau = 0$). Here we took the diffusion coefficient of $D_0 = 2 \times 10^{29}$ cm^2 s^{-1}.

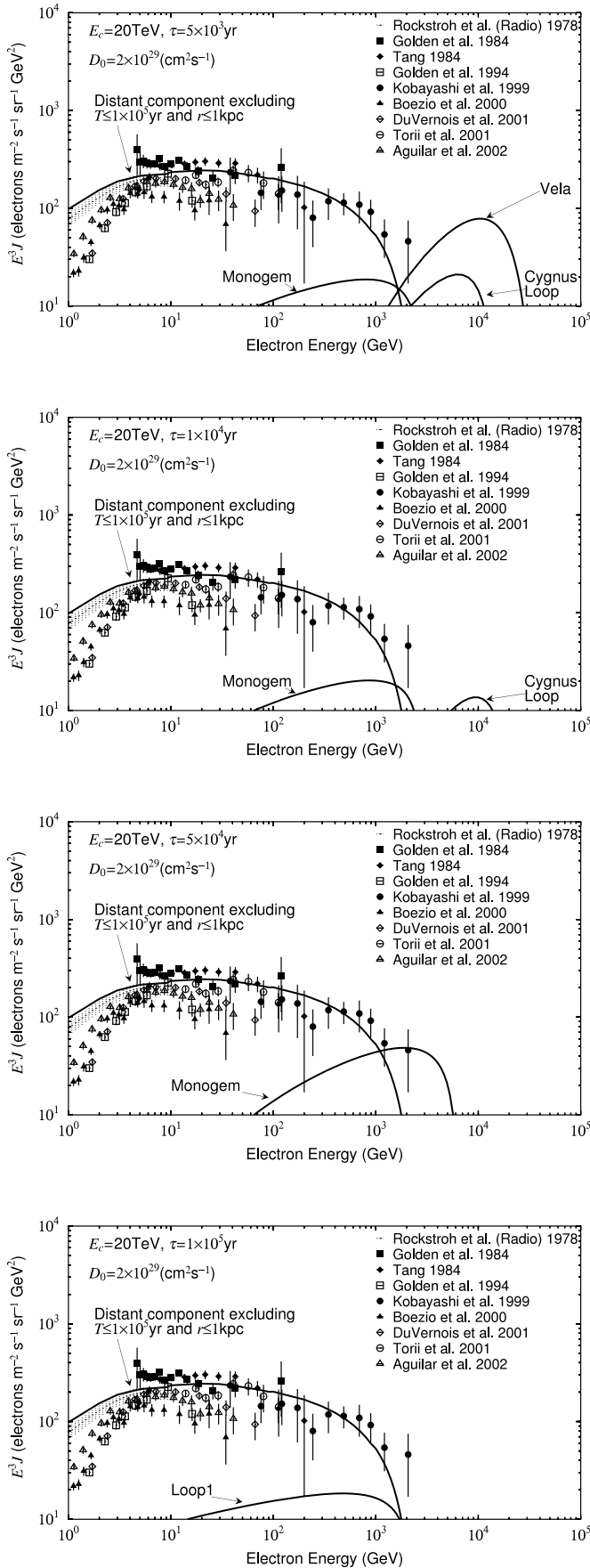FIG. 5.—Calculated energy spectra with $D_0 = 2 \times 10^{29}$ cm^2 s^{-1} and a cutoff of $E_c = 20$ TeV for the burstlike release at $\tau = 5 \times 10^3$, 1×10^4, 5×10^4, and 1×10^5 yr, respectively.
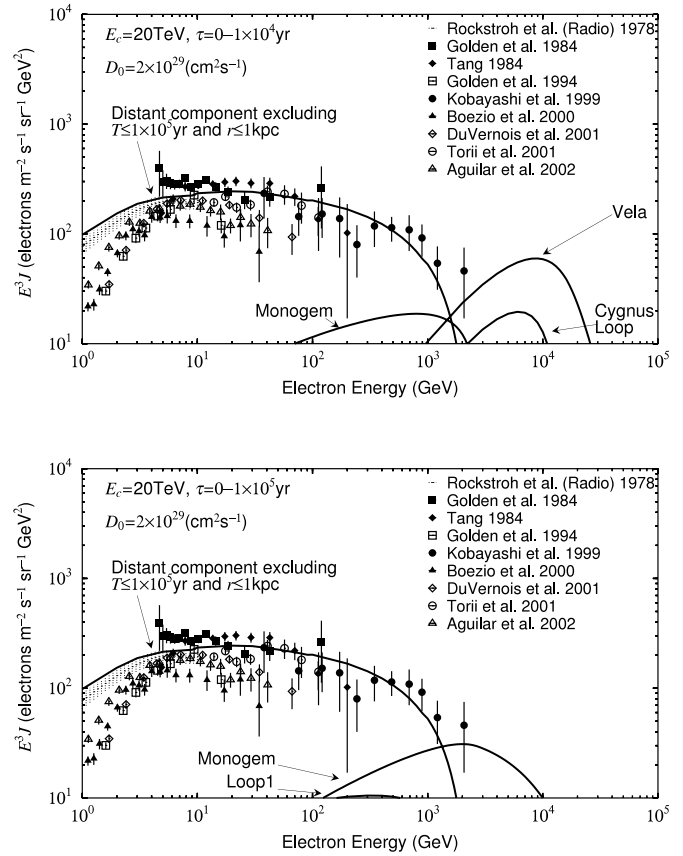
FIG. 6.—Calculated energy spectra with $D_0 = 2 \times 10^{29}$ cm^2 s^{-1} and a cutoff of $E_c = 20$ TeV for the continuous release time of $\tau = (0-1) \times 10^4$ and $(0-1) \times 10^5$ yr, respectively.

explosion determines which SNRs contribute cosmic-ray electrons in the TeV region. For $\tau = 0$ and $\tau = 5 \times 10^3$ yr, the energy spectra are similar to each other, and the Vela SNR is the most dominant source in the TeV region. For $\tau = 1 \times 10^4$ to 5×10^4 yr, the Cygnus Loop and the Monogem SNR are dominant, and for $\tau = 1 \times 10^5$ yr there are no dominant known sources in the TeV region. We can see that some combinations of parameters [e.g., $D = 5 \times 10^{29} (E/\text{TeV})^{0.3}$ cm^2 s^{-1}, $\tau = 0$, and $E_c = \infty$] are already ruled out even by the limited existing data. It should also be noted that if the magnetic field strength inside the remnant is higher, the lifetime of electrons becomes shorter and the flux of electrons becomes smaller after the delayed liberation in the TeV region.

Besides such primary electrons accelerated in SNRs, the observed cosmic-ray electron flux includes secondary electrons, produced mainly by interactions of cosmic-ray protons and nuclei with interstellar gas. The secondaries are mostly decay products of charged pions produced in interactions, i.e., $\pi^{\pm} \rightarrow \mu^{\pm} \rightarrow e^{\pm}$. As positrons are produced by this process, we can estimate the intensity of secondaries relative to primaries to be $\sim 10\%$ at 10 GeV from the observed ratio of e^+ to $e^- + e^+ \sim 5\%$ at 10 GeV (Barwick et al. 1997; Boezio et al. 2000). The spectral index $\gamma = 2.7$ for secondaries is the same as the index of the parent cosmic-ray protons and nuclei. This index is larger than that of primary electrons at the source, which is ~ 2.4 in the TeV region. Since the intensity relative to primary electrons decreases with increasing energy as $(E/10 \text{ GeV})^{\sim 2.4 - 2.7} = (E/10 \text{ GeV})^{\sim -0.3}$, the relative intensity of secondaries becomes $\sim 2.5\%$ at 1 TeV. This suggests

that the intensity of the secondary electrons is negligible compared to primary electrons in the energy range of interest here.

Next we estimate the degree of anisotropies from the specific sources in TeV region. Let $N_i(E, \mathbf{r}_i, t_i)$ be the contribution to the local density of cosmic-ray electrons at energy E from a source located at $\mathbf{r}_i$ and of age t_i. The anisotropy parameter Δ_i due to the density gradient of electrons is given by

$$\Delta_i \equiv \frac{I_{\max} - I_{\min}}{I_{\max} + I_{\min}} = \frac{3D}{c} \frac{\nabla N_i}{N_i} = \frac{3r_i}{2ct_i} \qquad (14)$$

for an individual source, where $I_{\max}$ and $I_{\min}$ are the maximum and minimum electron intensity in all directions (Shen & Mao 1971; Ptuskin & Ormes 1995). For example, the anisotropy of electrons for Vela with $\tau = 0$ is estimated to be 13%, where $r_i = 300$ pc and $t_i = 1.1 \times 10^4$ yr. The anisotropy becomes larger if we include the effect of the delay of the release time from SNRs.

In this paper, it is demonstrated that measurements of the energy spectrum of electrons in the TeV region are crucial to detect the unique effects of nearby sources as described above. If we observe pronounced features in the shape of the spectrum, together with anisotropy toward the nearby SNRs, we would confirm the nearby SNRs as the main contributors to electrons in the TeV region. We can also perform a more detailed analysis for the release time of electrons, cutoff energy, output energy, diffusion coefficient, and so on. The effect of the spatial extent of evolved SNRs on the flux and anisotropy may be important if the extent is quite large.

High-energy cosmic-ray electrons are the most powerful probe to help us identify the origin of cosmic rays. However, at present, only emulsion chamber data are available in the energy region of 1−2 TeV. To make significant additional observations on electrons in this region, not only balloon flight experiments with long exposures but also new experimental programs such as CALET on the International Space Station (Torii et al. 2002) are promising to observe the electron spectrum and anisotropy in TeV region with high statistical accuracy. Such direct observations will reveal the origin of cosmic-ray electrons in this energy region and also bring us important information on the sources, acceleration, and propagation of cosmic-ray electrons.

APPENDIX A

RELATION BETWEEN THE THREE-DIMENSIONAL SOLUTION OF THE DIFFUSION EQUATION WITHOUT BOUNDARIES, AND THE TWO-DIMENSIONAL SOLUTION WITH BOUNDARIES

In § 2.4, we gave solution (9) of the two-dimensional diffusion equation for a source of a power-law electron spectrum with boundaries defined by parallel planes. However, since it has the form of a series, it is tedious for numerical evaluation and difficult to understand the physical meaning of each term. We show that we can simplify the situation at high energies by substituting a three-dimensional solution without boundaries for the two-dimensional solution with boundaries. In this appendix, to find a general behavior of the solution, we treat a source of a power-law spectrum without an exponential cutoff. The arguments are valid for $E \ll E_c$, that is, $E <\sim 1$ TeV for $E_c = 10$–20 TeV.

Electrons propagate an average distance of $R = (2DT)^{1/2}$ during their lifetime of $T = 1/bE$. If the propagation distance is smaller than the Galactic halo thickness h, a three-dimensional solution without boundaries is applicable. Assuming that a source is located on the plane of the Galactic disk, the solution of the diffusion equation (4) is given by

$$N_e(E, r, t) = \frac{1}{(4\pi D_1)^{3/2}} e^{-r^2/(4D_1)} Q\left(\frac{E}{1 - bEt}\right) (1 - bEt)^{-2}, \qquad (A1)$$

where

$$D_1 = \int_E^{E/(1-bEt)} (1/b) D E^{-2} \, dE.$$

Here, assuming that the diffusion coefficient has the form $D = D_0 E^\delta$ and a source spectrum of the form $Q(E) = Q_0 E^{-\gamma}$, we have (e.g., Ginzburg & Ptuskin 1976 and references therein)

$$N_e(E, r, t) = \frac{Q_0}{(4\pi D_1)^{3/2}} e^{-r^2/(4D_1)} (1 - bEt)^{\gamma-2} E^{-\gamma}, \qquad (A2)$$

where

$$D_1 = \frac{D_0 \left[1 - (1 - bEt)^{1-\delta}\right]}{b(1 - \delta) E^{1-\delta}}.$$

Integrating the solution $N_e(E, r, t)$ (eq. [A2]) on r from 0 to ∞ and on t from 0 to $1/bE$, the electron flux J_3 (from sources assumed to be continuously and uniformly distributed in the Galactic disk) is given by

$$J_3(E) = \frac{c}{4\pi} f Q_0 \frac{E^{-\gamma-(1+\delta)/2}}{\left[4\pi D_0(1-\delta)b\right]^{1/2}} B\left[\frac{\gamma-1}{1-\delta}, \frac{1}{2}\right], \tag{A3}$$

where B is the beta function.

We compared this three-dimensional solution of J_3 with the two-dimensional solution of J with boundaries described in equation (10). Table 2 shows ratios of J_3 to J for halo thicknesses of 1–5 kpc and electron energies of 1 GeV to 10 TeV, taking the case of a diffusion coefficient of $D = 2 \times 10^{29}(E/\text{TeV})^{0.3}$ cm^2 s^{-1} as an example in the TeV energy region with equation (3) below 50 GeV. For larger halo thicknesses or electron energies, the differences between J_3 and J become smaller. For the case in which halo thickness $h = 3$ kpc, it is shown that the two solutions above 10 GeV region agree with each other within an error of 1%.

APPENDIX B

EVALUATION OF COSMIC-RAY ELECTRON FLUX FROM DISTANT SOURCES

We define the total flux of electrons as $J(E)$, the flux from distant source at large distances or relatively old ages as J_d, and the flux from nearby sources as J_n.

To avoid statistical fluctuations in the flux due to the small number of nearby sources, we evaluate J_d as shown in § 2.4 in the following:

$$J_d(E) = J(E) - J_n(E), \tag{B1}$$

where

$$J_n = \frac{c}{4\pi} \int_0^{T_0} dt \int_0^{R_0} d\rho f N_e(E, \rho, t) 2\pi\rho \tag{B2}$$

is equation (13) defined in § 2.4.

Then we have

$$\begin{aligned}
J_d(E) &= \frac{c}{4\pi}\left[\int_0^\infty dt \int_0^\infty d\rho f N_e(E, \rho, t)2\pi\rho - \int_0^{T_0} dt \int_0^{R_0} d\rho f N_e(E, \rho, t)2\pi\rho\right] \\
&= \frac{c}{4\pi}\left[\int_{T_0}^\infty dt \int_0^\infty d\rho f N_e(E, \rho, t)2\pi\rho + \int_0^{T_0} dt \int_{R_0}^\infty d\rho f N_e(E, \rho, t)2\pi\rho\right].
\end{aligned} \tag{B3}$$

The integrations are carried out in domains 1 and 2, where domain 1 is $T_0 < t < \infty$ and $0 < \rho < \infty$, and domain 2 is $0 < t < T_0$ and $R_0 < \rho < \infty$, respectively. Here we discuss how to find the appropriate values of R_0 and T_0 for separation of distant and nearby source components.

Taking the three-dimensional solution of equation (A2), the total flux $J(E)$ is given by equation (A3) as

$$J(E) = \frac{c}{4\pi} f Q_0 \frac{E^{-\gamma-(1+\delta)/2}}{\left[4\pi D_0(1-\delta)b\right]^{1/2}} B\left[\frac{\gamma-1}{1-\delta}, \frac{1}{2}\right], \tag{B4}$$

in the case of a power-law source spectrum, where B is the beta function. Then the energy spectrum extends with a power law of the form $E^{-\gamma-(1+\delta)/2}$ without cutoff, as is already known in the literatures (e.g., Berezinskii et al. 1990).

TABLE 2
RATIOS OF THE THREE-DIMENSIONAL SOLUTION WITHOUT BOUNDARIES J_3 TO THE TWO-DIMENSIONAL
SOLUTION WITH BOUNDARIES J FOR VARIOUS ENERGIES AND HALO THICKNESSES

h (kpc)	ELECTRON ENERGY				
	1 GeV	10 GeV	100 GeV	1 TeV	10 TeV
1.........	3.35	1.69	1.08	1.00	1.00
2.........	1.77	1.10	1.00	1.00	1.00
3.........	1.30	1.01	1.00	1.00	1.00
4.........	1.12	1.00	1.00	1.00	1.00
5.........	1.05	1.00	1.00	1.00	1.00

The first term in equation (B3) (domain 1) is given by

$$\frac{c}{4\pi} f Q_0 \frac{E^{-\gamma-(1+\delta)/2}}{[4\pi D_0 (1-\delta)b]^{1/2}} B\left[(1-bET_0)^{1-\delta}, \frac{\gamma-1}{1-\delta}, \frac{1}{2}\right], \tag{B5}$$

where B is the incomplete Beta function. The fraction of the flux from domain 1 to the total flux, i.e., (B5)/(B4), should be small enough for the justification on the separation of nearby sources from distant sources. Numerical value of the fraction (B5)/(B4) is less than a few percent when $T_0 = 1 \times 10^5$ yr and $E > 2$ TeV.

The contribution from domain 2 (the second term in eq. [B3]) is given by

$$\frac{c}{4\pi} f Q_0 \int_0^{T_0} dt (1-bEt)^{\gamma-2} \frac{E^{-\gamma}}{(4\pi D_1)^{1/2}} e^{-\left(R_0^2/4D_1\right)}. \tag{B6}$$

Replacing the variable t with x, as

$$x = \frac{1}{1-(1-bEt)^{1-\delta}},$$

the integration (B6) is reduced to

$$\frac{c}{4\pi} f Q_0 \frac{E^{-\gamma-(1+\delta)/2}}{[4\pi D_0 (1-\delta)b]^{1/2}} \int_{1/\left[1-(1-bET_0)^{1-\delta}\right]}^{\infty} dx (x-1)^{[(\gamma-2+\delta)/(1-\delta)]} x^{-1.5-[(\gamma-2+\delta)/(1-\delta)]} e^{-x_0 x}, \tag{B7}$$

where

$$x_0 = \frac{R_0^2 bE(1-\delta)}{4D_0 E^\delta} = \frac{1}{2}\left(\frac{R_0}{R_a}\right)^2,$$

with

$$R_a = \left\{2D_0 E^\delta/[bE(1-\delta)]\right\}^{1/2}.$$

The physical meaning of R_a is that it represents almost the average distance traveled by diffusion of electrons with energy E.

The upper limit of the integration in equation (B7) is obtained by putting the lower boundary of x to be 1.0, i.e., $T_0 = 1/bE$. The integral of equation (B7) is then given by the confluent hypergeometric functions, as

$$\Gamma\left(\frac{\gamma-1}{1-\delta}\right)\left\{\frac{\sqrt{\pi} {}_1F_1[-0.5-(\gamma-2+\delta)/(1-\delta),\ 0.5,\ -x_0]1}{\Gamma[1.5+(\gamma-2+\delta)/(1-\delta)]} - \frac{2\sqrt{\pi}x_0^{0.5} {}_1F_1[-(\gamma-2+\delta)/(1-\delta),\ 1.5,\ -x_0]}{\Gamma[(\gamma-1)/(1-\delta)]}\right\}, \tag{B8}$$

or in another form of the confluent hypergeometric function U, as

$$e^{-x_0}\Gamma\left(\frac{\gamma-1}{1-\delta}\right) U\left(\frac{\gamma-1}{1-\delta},\ 0.5,\ x_0\right). \tag{B9}$$

TABLE 3
RELATIVE CONTRIBUTION F OF THE FLUX AT $E = 1/bT_0$ IN DOMAIN
2 $(0 < t < T_0,\ R_0 < \rho < \infty)$ TO THE TOTAL FLUX

$x_0 = (1/2)(R_0/R_a)^{2\text{a}}$	F
0.2	0.2722
0.4	0.1481
0.6	0.0901
0.8	0.0580
1.0	0.0387
1.2	0.0265
1.4	0.0185
1.6	0.0131
1.8	0.0094
2.0	0.0068

[a] See text for the definition of the domain and the parameter x_0.

If the numerical value of $(\gamma - 2 + \delta)/(1 - \delta)$ is an integer, the integration in equation (B7) can be performed without imposing any conditions on T_0. For example, if we take $\gamma = 2.4$ and $\delta = 0.3$, we have $(\gamma - 2 + \delta)/(1 - \delta) = 1.0$. Then the integration of equation (B7) is carried out, and we have

$$\frac{c}{4\pi} f Q_0 \frac{E^{-3.05}}{[4\pi D_0 (0.7) b]^{1/2}} \left\{ x_0^{0.5} \Gamma\left[-0.5, \ \frac{x_0}{1 - (1 - bET_0)^{0.7}} \right] - x_0^{1.5} \Gamma\left[-1.5, \ \frac{x_0}{1 - (1 - bET_0)^{0.7}} \right] \right\}, \qquad \text{(B10)}$$

where Γ is the incomplete gamma function.

Here we define the ratio F of the flux in domain 2 to the total flux as

$$F = \frac{3}{4} \left\{ x_0^{0.5} \Gamma\left[-0.5, \ \frac{x_0}{1 - (1 - bET_0)^{0.7}} \right] - x_0^{1.5} \Gamma\left[-1.5, \ \frac{x_0}{1 - (1 - bET_0)^{0.7}} \right] \right\}, \qquad \text{(B11)}$$

where we used $B(2, \ 1/2) = 4/3$ for the total flux from equation (B4). Here F is a function of x_0 and gives the relative contribution to the total flux for a given value of bET_0 from sources in domain 2. The numerical values of F is listed in Table 3. As shown in Table 3, we need to take $x_0 > 0.8$ to reduce the contribution from sources in domain 2 to less than 6% of the total flux. This means we need to take the boundaries of domain 2 as $R_0 > \sqrt{2} R_a$. The average travel distance R_a is evaluated as 0.5–0.8 kpc at $E = 2$ TeV depending on the values of D_0 here we adopted. Thus, if we put 1 kpc for R_0, the contribution from domain 2 gives less than 6% for $E > 2$ TeV.

In summary, the treatment of separation of nearby and distant sources is justified in the energy region beyond $\sim$2 TeV if we set $R_0 = 1$ kpc and $T_0 = 1 \times 10^5$ yr.

REFERENCES

Aguilar, M., et al. 2002, Phys. Rep., 366, 331
Aharonian, F. A., Atoyan, A. M., & Völk, H. J. 1995, A&A, 294, L41
Allen, G. E., et al. 1997, ApJ, 487, L97
Ambrosio, M., et al. 2003, Phys. Rev. D, 67, 042002
Aschenbach, B. 1998, Nature, 396, 141
Atoyan, A. M., Aharonian, F. A., & Völk, H. J. 1995, Phys. Rev. D, 52, 3265
Barwick, S. W., et al. 1997, ApJ, 482, L191
Berezinskii, V. S., Bulanov, S. V., Dogiel, V. A., Ginzburg, V. L., & Ptuskin, V. S. 1990, in Astrophysics of Cosmic Rays, ed. Ginzburg, V. L. (North-Holland: Amsterdam), 1
Beuermann, K., Kanbach, G., & Berkhuijsen, E. M. 1985, A&A, 153, 17
Blair, W. P., Sankrit, R., Raymond, J. C., & Long, K. S. 1999, AJ, 118, 942
Blumenthal, G. R., & Gould, R. J. 1970, Rev. Mod. Phys., 42, 237
Boezio, M., et al. 2000, ApJ, 532, 653
Braun, R., Goss, W. M., & Lyne, A. G. 1989, ApJ, 340, 355
Butt, Y. M., Torres, D. F., Romero, G. E., Dame, T., & Combi, J. A. 2002, Nature, 418, 499
Caraveo, P. A., Bignami, G. F., Mignami, R. P., & Taff, L. G. 1996, ApJ, 461, L91
Caraveo, P. A., De Luca, A., Mignami, R. P., & Bignami, G. F. 2001, ApJ, 561, 930
Cha, A. N., Sembach, K. R., & Danks, A.C 1999, ApJ, 515, L25
Cowsik, R., & Lee, M. A. 1979, ApJ, 228, 297
Dorfi, E. A. 2000, Ap&SS, 272, 227
DuVernois, M. A., et al. 2001, ApJ, 559, 296
Egger, R. J., & Aschenbach, B. 1995, A&A, 294, L25
Engelmann, J. J., et al. 1990, A&A, 233, 96
Enomoto, R., et al. 2002, Nature, 416, 823
Erlykin, A. D., & Wolfendale, A. W. 2002, J. Phys. G, 28, 359
Ferriere, K. M. 2001, Rev. Mod. Phys., 73, 1031
Furukawa, M., et al. 2003, Proc. 28th Int. Cosmic-Ray Conf. (Tsukuba), 4, 1877
Gaisser, T. K. 1990, Cosmic Rays and Particle Physics (Cambridge: Cambridge Univ. Press)
———. 2000, preprint (astro-ph/0011524)
Ginzburg, V. L., & Ptuskin, V. S. 1976, Rev. Mod. Phys., 48, 161
Golden, R. L., et al. 1984, ApJ, 287, 622
———. 1994, ApJ, 436, 769
Green, D. A. 1988, Ap&SS, 148, 3
Hendrick, S. P., & Reynolds, S. P. 2001, ApJ, 559, 903
Iyudin, A. F., et al. 1998, Nature, 396, 142

Jokipii, J. R., & Meyer, P. 1968, Phys. Rev. Lett., 20, 752
Jones, F. C., Lukasiak, A., & Ptuskin, V. 2001, ApJ, 547, 264
Keohane, J. W., Petre, R., Gotthelf, E. V., Ozaki, M., & Koyama, K. 1997, ApJ, 484, 350
Kobayashi, T., et al. 1999, Proc. 26th Int. Cosmic-Ray Conf. (Salt Lake City), 3, 61
Kodaira, K. 1974, PASJ, 26, 255
Koyama, K., et al. 1995, Nature, 378, 255
———. 1997, PASJ, 49, L7
Leahy, D. A., & Aschenbach, B. 1996, A&A, 315, 260
Leahy, D. A., & Xinji, W. 1989, PASP, 101, 607
Lukasiak, A., Ferrando, P., McDonald, F. B., & Webber, W. R. 1994, ApJ, 423, 426
Mathis, J. S., Mezger, P. G., & Panagia, N. 1983, A&A, 128, 212
Milne, D. K. 1968, Australian J. Phys., 21, 201
Minkowski, R. 1958, Rev. Mod. Phys., 30, 1048
Miyata, E., Tsunemi, H., Pisarski, R., & Kissel, S. E. 1994, PASJ, 46, L101
Nishimura, J., Fujii, M. & Taira, T. 1979, Proc. 16th Int. Cosmic-Ray Conf. (Kyoto), 1, 488
Nishimura, J., et al. 1980, ApJ, 238, 394
Pohl, M., & Esposito, J. A. 1998, ApJ, 507, 327
Plucinsky, P. P., et al. 1996, ApJ, 463, 224
Ptuskin, V. S., & Ormes, J. F. 1995, Proc. 24th Int. Cosmic-Ray Conf. (Rome), 3, 56
Reimer, D., & Pohl, M. 2002, A&A, 390, L43
Reynolds, S. P. 1996, ApJ, 459, L13
Reynolds, S. P., & Keohane, J. W. 1999, ApJ, 525, 368
Rockstroh, J. M., & Webber, W. R. 1978, ApJ, 224, 677
Shen, C. S. 1970, ApJ, 162, L181
Shen, C. S., & Mao, C. Y. 1971, Astrophys. Lett., 9, 169
Slane, P., et al. 1999, ApJ, 525, 357
———. 2001, ApJ, 548, 814
Strom, R. G. 1994, A&A, 288, L1
Sturner, S. J., Skibo, J. G., Dermer, C. D., & Mattox, J. R. 1997, ApJ, 490, 619
Tang, K. K. 1984, ApJ, 278, 881
Tanimori, T., et al. 1998, ApJ, 497, L25
Tatematsu, K., Fukui, Y., Landecker, T. L., & Roger, R. S. 1990, A&A, 237, 189
Taylor, J. H., & Cordes, J. M. 1993, ApJ, 411, 674
Torii, S., et al. 2001, ApJ, 559, 973
———. 2002, Nucl. Phys. B, 113, 103